C5—C6	1.520 (4)	C15—N16	1.459 (3)
C6—C7	1.542 (4)	N16—C17	1.455 (3)
C7—C8	1.528 (4)	C18—N19	1.136 (4)
C7—C17	1.530 (4)		
C2—N1—C6	113.5 (2)	C9—C8—C7	105.6 (2)
C2—N1—C10	112.2 (2)	C8—C9—C10	109.3 (2)
C6—N1—C10	110.8 (2)	C8—C9—C11	110.8 (2)
N1—C2—C18	110.4 (2)	C10—C9—C11	112.8 (2)
N1—C2—C20	111.6 (2)	N1—C10—C9	112.2 (2)
C18—C2—C20	108.1 (2)	N16—C11—C12	108.8 (2)
N1—C2—C3	110.2 (2)	N16—C11—C9	110.6 (2)
C18—C2—C3	107.7 (2)	C12—C11—C9	111.9 (2)
C20—C2—C3	108.8 (2)	C13—C12—C11	112.6 (3)
C4—C3—C2	112.3 (2)	C14—C13—C12	111.1 (3)
C5—C4—C3	108.8 (2)	C15—C14—C13	110.5 (3)
C4—C5—C6	112.9 (2)	N16—C15—C14	111.0 (3)
N1—C6—C5	112.3 (2)	C17—N16—C15	110.8 (2)
N1—C6—C7	109.5 (2)	C17—N16—C11	110.4 (2)
C5—C6—C7	110.9 (2)	C15—N16—C11	111.7 (2)
C8—C7—C17	109.0 (2)	N16—C17—C7	112.7 (2)
C8—C7—C6	109.0 (2)	N19—C18—C2	178.9 (3)
C17—C7—C6	113.0 (2)		

Data collection: *Kuma KM-4 User's Guide* (Kuma, 1992). Cell refinement: *Kuma KM-4 User's Guide*. Data reduction: *Kuma KM-4 User's Guide*. Program(s) used to solve structure: *SHELXS86* (Sheldrick, 1990). Program(s) used to refine structure: *SHELXL93* (Sheldrick, 1993). Molecular graphics: *Stereochemical Workstation Operation Manual* (Siemens, 1989). Software used to prepare material for publication: *SHELXL93* (Sheldrick, 1993).

Lists of structure factors, anisotropic displacement parameters, H-atom coordinates, complete geometry, including bond distances and angles involving H atoms, and torsion angles have been deposited with the IUCr (Reference: BK1085). Copies may be obtained through The Managing Editor, International Union of Crystallography, 5 Abbey Square, Chester CH1 2HU, England.

References

Borowiak, T., Bokii, N. G. & Struchkov, Yu. T. (1973). *Zh. Strukt. Khim.* **14**, 387–388.

Katrusiak, A., Figas, E., Kałuski, Z. & Lesiewicz, D. (1989). *Acta Cryst.* C**45**, 1758–1760.

Klyne, S., Scopes, P. N., Thomas, R. N., Skolik, J., Gawroński, J. & Wiewiórowski, M. (1974). *J. Chem Soc. Perkin Trans.* 1, pp. 2565–2570.

Kubicki, M., Borowiak, T. & Boczoń, W. (1991). *J. Crystallogr. Spectrosc. Res.* **21**, 575–579.

Kuma (1992). *Kuma KM-4 User's Guide*. Version 6.0. Kuma Diffraction, Wrocław, Poland.

Sheldrick, G. M. (1990). *Acta Cryst.* A**46**, 467–473.

Sheldrick, G. M. (1993). *SHELXL93. Program for Crystal Structure Refinement*. Univ. of Göttingen, Germany.

Siemens (1989). *Stereochemical Workstation Operation Manual*. Release 3.4. Siemens Analytical X-ray Instruments Inc., Madison, Wisconsin, USA.

Skolik, J., Krueger, P. J. & Wiewiórowski, M. (1970). *J. Mol. Struct.* **5**, 461–475.

Acta Cryst. (1995). C**51**, 1160–1164

Conformationally Defined Cyclohexyl Carnitine Analogs

WAYNE J. BROUILLETTE, GARY M. GRAY* AND ASHRAF SAEED

Department of Chemistry, University of Alabama at Birmingham, Birmingham, AL 35294-1240, USA

(*Received* 24 *January* 1994; *accepted* 9 *September* 1994)

Abstract

Three diastereoisomers of racemic (3-carboxy-2-hydroxy-1-cyclohexyl)trimethylammonium chloride [$C_{10}H_{20}NO_3^+.Cl^-$; (1*S*,2*S*,3*S*) (2), (1*R*,2*S*,3*S*) (3) and (1*S*,2*R*,3*S*) (4)] were designed as rigid analogs for different low-energy conformational states of carnitine [(1), (3-carboxy-2-hydroxy-1-propyl)trimethylammonium chloride]. Structures (2)–(4) all assume a chair conformation in the solid state, in which the bulky trimethylammonio group occupies the equatorial position. As such, the orientations about C2—C3 in (2), (3) and (4) are all essentially the same as that found for (1) in the solid state (torsion angles for C1—C2—C3—N1 near 180°), while the orientations about C1—C2 in (2)–(4) are such that each diastereoisomer contains a different one of the three possible low-energy staggered conformations predicted for (1) in solution. Comparisons between (1) and (2)–(4) in the solid state revealed that diastereoisomers (2), (3) and (4) provide rigid models for the major low-energy conformations of carnitine.

Comment

(*R*)-Carnitine (1) is important in cellular metabolism as a substrate for several different carnitine acyltransferases. Structure (1) is conformationally flexible and determining the protein-bound conformation for (1) with each of the acyltransferases is of considerable pharmacological interest. Studies by others (Colucci & Gandour, 1988) have suggested that protein-bound (1) contains a *gauche* relationship between N1 and O3 [atoms were numbered as in (2)–(4) for easy comparison]. This conformation about C2—C3 also exists in the crystal structure of (1) (Tomita, Urabe, Kim & Fujiwara, 1974) and is favored in solution (Colucci, Gandour & Mooberry, 1986). However, the protein-bound conformation for (1) about C1—C2 has not been determined and two of the three possible low-energy staggered conformations are nearly equally favored in solution (Colucci, Gandour & Mooberry, 1986). As part of a study to address this question, we synthesized racemic cyclohexyl carnitine analogs (2), (3) and (4) (Brouillette, Saeed, Abuelyaman, Hutchison, Wolkowicz & McMillin, 1994).

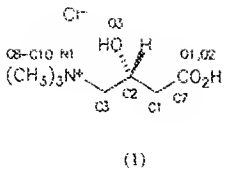

(1)

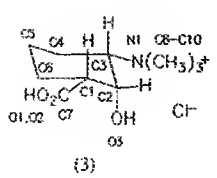

(3)

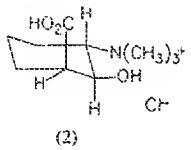

(2)

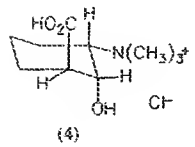

(4)

It was anticipated that structures (2)–(4) would each exist in a 'locked' chair form, with the bulky trimethylammonio group occupying the equatorial position, thus providing conformationally rigid analogs of (1). Consequently, (2)–(4) each contain the desired *gauche* relationship between N1 and O3 but different low-energy staggered conformations about C1—C2. In order to confirm the relative stereochemical assignments and to assure that diastereoisomer (4), which contains two substituents in the axial position, does not favor a twisted-boat conformation in the solid state, the crystal structures for the hydrochloride salts of (2), (3) and (4) were solved.

Observed bond angles and distances in racemic (2), (3) and (4) are in relatively good agreement with those for (*R*)-carnitine (1). The exceptions are that the N1—C3 bond distance is longer and the N1—C3—C2 bond angle is narrower for racemates (2)–(4), presumably due to extra steric crowding from C4.

Among the selected torsion angles in Table 2, those given for (1) (except C2—C1—C7—O2) are of greatest interest since they define the spatial relationship between the carboxyl, hydroxyl and ammonio groups, which for (1) are involved in enzyme binding or enzymatic reaction. Comparison of these torsion angles indicates that the conformation of (3) most closely resembles that of (1) in the solid state, except that in (3) C7—C1—C2—O3 is about 23° smaller than in (1). The large deviation between (1) and (3) for C2—C1—C7—O2 (the carboxyl group orientation) likely results from differences in crystal packing forces. Racemic (2) and (4), like (3), also maintain the desired *gauche* relationship between N1 and O3. The deviation of the O3—C2—C3—N1 torsion angle from the ideal angle of 60° is largest in (4), which has two axial groups. Structures (2)–(4) each exhibit different low-energy staggered conformations about C1—C2 that were earlier predicted to predominate for (1) in solution (Colucci, Gandour & Mooberry, 1986), and the C7—C1—C2—O3 torsion angles are, in all cases, relatively close to the desired torsion angles of 60 or 180°. Structures (2)–(4) thus provide rigid structural models for the major low-energy conformations of carnitine that are observed in the solid state and in solution.

For structures (2) and (3), intermolecular hydrogen bonding is similar to that observed for carnitine hydrochloride (1) (Tomita, Urabe, Kim & Fujiwara, 1974). In (1)–(3) the chloride ion mediates interactions between molecules by accepting a hydrogen bond from O1 of one molecule and O3 of the adjacent molecule. In structure (4) only the former hydrogen bond is observed.

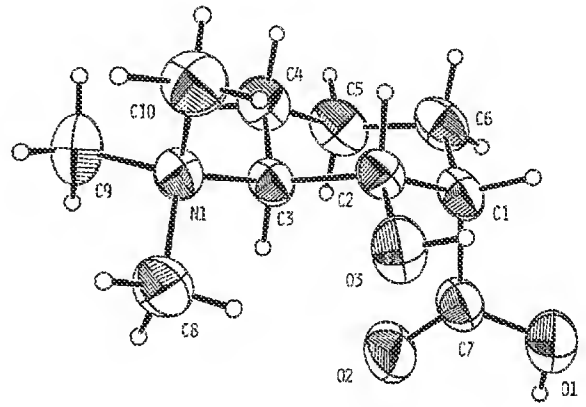

(*a*)

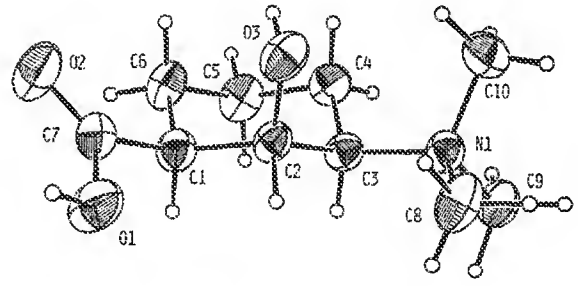

(*b*)

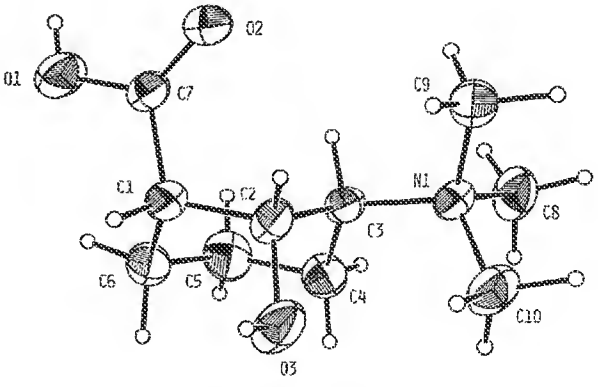

(*c*)

Fig. 1. Atom-numbering scheme and displacement ellipsoids drawn at the 50% probability level for (*a*) (2), (*b*) (3) and (*c*) (4). H atoms are drawn with arbitrary radii.

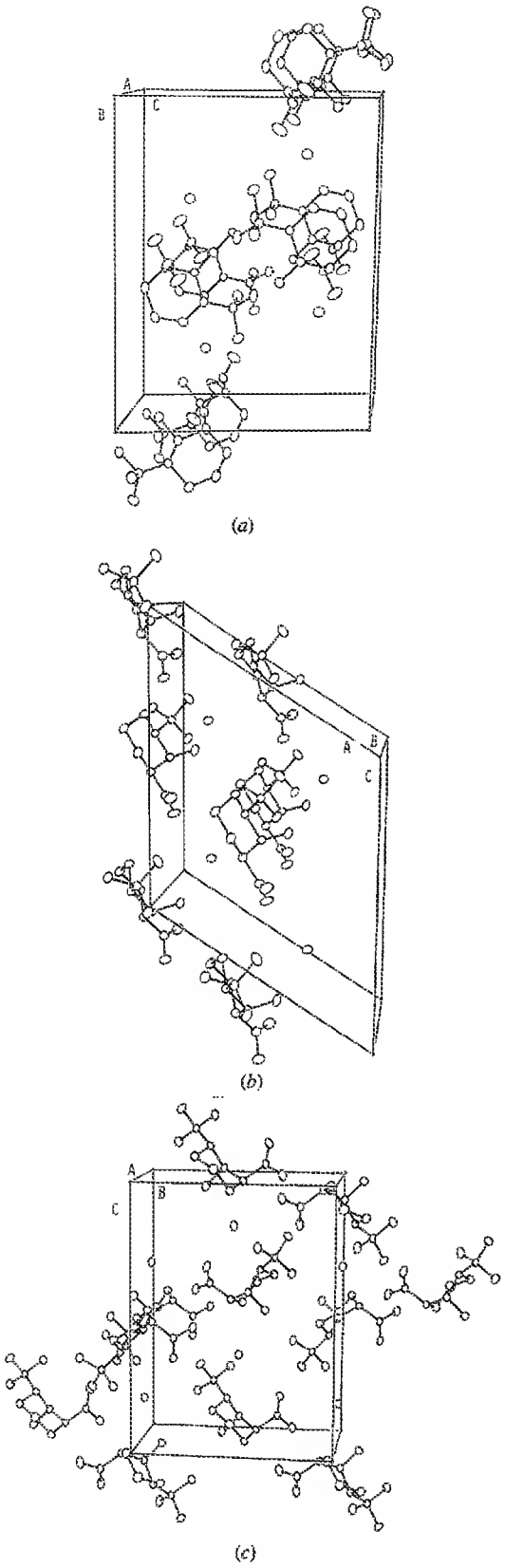

Fig. 2. The unit cell for (*a*) (2), (*b*) (3) and (*c*) (4).

Experimental

Crystals of racemic (2)–(4), which were synthesized by methods developed in our laboratory, were prepared by the slow vapor diffusion of diethyl ether into a saturated solution in ethanol. Melting points were (2) 522–522.5, (3) 479.5–481 and (4) 510–511 K. Crystals were cut to the appropriate sizes and then mounted on glass fibers with Super Glue gel.

Structure (2)

Crystal data

$C_{10}H_{20}NO_3^+.Cl^-$
$M_r = 237.73$
Monoclinic
$P2_1/n$
$a = 6.418\ (1)$ Å
$b = 15.864\ (3)$ Å
$c = 12.269\ (2)$ Å
$\beta = 102.38\ (1)°$
$V = 1220.2\ (6)$ Å^3
$Z = 4$
$D_x = 1.293$ Mg m^{-3}
Cu $K\alpha$ radiation
$\lambda = 1.5418$ Å
Cell parameters from 25 reflections
$\theta = 25–35°$
$\mu = 2.73$ mm^{-1}
$T = 296$ K
Needle cut into block
0.55 × 0.49 × 0.32 mm
Colorless

Data collection

Enraf–Nonius CAD-4 diffractometer
ω–2θ scans
Absorption correction: empirical
$T_{min} = 0.872$, $T_{max} = 0.999$
2735 measured reflections
2665 independent reflections
1981 observed reflections [$I \geq 3\sigma(I)$]
$\theta_{max} = 74°$
$h = -8 \rightarrow 8$
$k = 0 \rightarrow 19$
$l = 0 \rightarrow 15$
3 standard reflections
frequency: 60 min
intensity decay: −4.0%

Refinement

Refinement on F
$R = 0.0507$
$wR = 0.0712$
$S = 2.172$
1981 reflections
195 parameters
Only coordinates of H atoms refined (O—H 0.81–0.87, C—H 0.85–1.05 Å)
$w = 1/\sigma^2(F_o)$
$(\Delta/\sigma)_{max} = 0.02$
$\Delta\rho_{max} = 0.251$ e Å^{-3}
$\Delta\rho_{min} = -0.301$ e Å^{-3}
Extinction correction: Zachariasen (1963)
Extinction coefficient: $1.5\ (3) \times 10^{-6}$
Atomic scattering factors from Cromer & Waber (1974)

Structure (3)

Crystal data

$C_{10}H_{20}NO_3^+.Cl^-$
$M_r = 237.73$
Monoclinic
Cc
$a = 12.390\ (1)$ Å
$b = 8.245\ (2)$ Å
$c = 13.732\ (1)$ Å
$\beta = 121.543\ (9)°$
$V = 1195.6\ (3)$ Å^3
$Z = 4$
$D_x = 1.321$ Mg m^{-3}
Cu $K\alpha$ radiation
$\lambda = 1.5418$ Å
Cell parameters from 25 reflections
$\theta = 25–35°$
$\mu = 2.79$ mm^{-1}
$T = 295$ K
Needle cut into block
0.65 × 0.62 × 0.46 mm
Colorless

Data collection

Enraf–Nonius CAD-4 diffractometer
ω–2θ scans
Absorption correction: empirical
T_{min} = 0.899, T_{max} = 0.998
1301 measured reflections
1272 independent reflections

1242 observed reflections [$I \geq 3\sigma(I)$]
θ_{max} = 74°
$h = -15 \rightarrow 0$
$k = 0 \rightarrow 10$
$l = -17 \rightarrow 17$
3 standard reflections
frequency: 60 min
intensity decay: −0.1%

Refinement

Refinement on F
R = 0.025 (or 0.034)
wR = 0.0332 (or 0.054)
S = 1.415 (or 1.21)
1242 reflections
197 parameters
Only coordinates of H atoms refined (O—H 0.76–0.79, C—H 0.89–1.14 Å)
$w = 1/\sigma^2(F_o)$

$(\Delta/\sigma)_{max}$ = 0.01
$\Delta\rho_{max}$ = 0.111 e Å^{-3}
$\Delta\rho_{min}$ = −0.043 e Å^{-3}
Extinction correction: Zachariasen (1963)
Extinction coefficient: 9.1 (7) × 10^{-6}
Atomic scattering factors from Cromer & Waber (1974)

Structure (4)

Crystal data

$C_{10}H_{20}NO_2^+.Cl^-$
M_r = 237.73
Orthorhombic
$P2_12_12_1$
a = 7.123 (2) Å
b = 11.237 (2) Å
c = 14.989 (1) Å
V = 1199.7 (4) Å^3
Z = 4
D_x = 1.316 Mg m^{-3}

Cu $K\alpha$ radiation
λ = 1.5418 Å
Cell parameters from 25 reflections
θ = 25–35°
μ = 2.78 mm^{-1}
T = 296 K
Needle cut into block
0.73 × 0.67 × 0.60 mm
Colorless

Data collection

Enraf–Nonius CAD-4 diffractometer
ω–2θ scans
Absorption correction: empirical
T_{min} = 0.940, T_{max} = 1.00
1468 measured reflections
1441 independent reflections

1394 observed reflections [$I \geq 3\sigma(I)$]
θ_{max} = 74°
$h = -8 \rightarrow 0$
$k = -14 \rightarrow 0$
$l = 0 \rightarrow 18$
3 standard reflections
frequency: 60 min
intensity decay: none

Refinement

Refinement on F
R = 0.030 (or 0.045)
wR = 0.041 (or 0.063)
S = 1.92 (or 2.97)
1394 reflections
197 parameters
Only coordinates of H atoms refined (O—H 0.74–0.80, C—H 0.82–1.09 Å)
$w = 1/\sigma^2(F_o)$

$(\Delta/\sigma)_{max}$ = 0.02
$\Delta\rho_{max}$ = 0.180 e Å^{-3}
$\Delta\rho_{min}$ = −0.239 e Å^{-3}
Extinction correction: Zachariasen (1963)
Extinction coefficient: 1.36 (3) × 10^{-5}
Atomic scattering factors from Cromer & Waber (1974)

Table 1. *Fractional atomic coordinates and equivalent isotropic displacement parameters* (Å^2)

$B_{eq} = (4/3)\sum_i\sum_j\beta_{ij}\mathbf{a}_i.\mathbf{a}_j$.

	x	y	z	B_{eq}
Structure (2)				
Cl	0.1149 (1)	0.17031 (5)	0.27404 (7)	4.45 (2)
O1	−0.4738 (4)	0.0785 (2)	0.3517 (3)	6.41 (7)
O2	−0.5833 (4)	−0.0332 (2)	0.2520 (3)	6.85 (7)
O3	−0.1754 (4)	0.0226 (1)	0.1510 (2)	4.35 (5)
N1	−0.1685 (4)	−0.1512 (2)	0.0711 (2)	3.28 (5)
C1	−0.2087 (4)	−0.0190 (2)	0.3360 (2)	3.48 (5)
C2	−0.1299 (4)	−0.0438 (2)	0.2307 (2)	3.13 (5)
C3	−0.2248 (4)	−0.1281 (2)	0.1836 (2)	2.98 (5)
C4	−0.1569 (5)	−0.1958 (2)	0.2726 (3)	3.96 (6)
C5	−0.2450 (6)	−0.1735 (2)	0.3756 (3)	4.60 (7)
C6	−0.1636 (5)	−0.0888 (2)	0.4237 (2)	4.28 (7)
C7	−0.4432 (5)	0.0061 (2)	0.3069 (3)	3.83 (6)
C8	−0.3112 (6)	−0.1023 (2)	−0.0210 (3)	4.93 (8)
C9	−0.2070 (6)	−0.2431 (2)	0.0458 (3)	5.12 (8)
C10	0.0591 (5)	−0.1335 (2)	0.0693 (3)	4.65 (7)
HO1	−0.602 (7)	0.080 (3)	0.338 (4)	10†
HO3	−0.107 (5)	0.068 (2)	0.177 (3)	5.8†
Structure (3)				
Cl	0.800	0.55262 (7)	0.800	3.93 (1)
O1	0.4919 (2)	1.1395 (2)	0.7411 (1)	4.55 (3)
O2	0.4699 (2)	0.9042 (2)	0.6537 (1)	4.54 (4)
O3	0.4059 (1)	1.2318 (2)	0.4771 (1)	3.36 (3)
N1	0.5599 (1)	1.4934 (2)	0.4574 (1)	2.72 (3)
C1	0.5988 (2)	1.1143 (3)	0.6419 (2)	2.89 (4)
C2	0.5312 (2)	1.2633 (2)	0.5667 (1)	2.54 (4)
C3	0.6153 (2)	1.3355 (2)	0.5259 (1)	2.44 (4)
C4	0.6464 (2)	1.2127 (3)	0.4617 (2)	3.08 (4)
C5	0.7172 (2)	1.0703 (3)	0.5410 (2)	3.46 (4)
C6	0.6372 (2)	0.9907 (3)	0.5826 (2)	3.32 (4)
C7	0.5141 (2)	1.0381 (3)	0.6784 (2)	3.11 (4)
C8	0.4944 (2)	1.5919 (3)	0.5029 (2)	3.83 (5)
C9	0.6686 (2)	1.5922 (3)	0.4698 (2)	3.38 (4)
C10	0.4696 (3)	1.4628 (3)	0.3326 (2)	4.49 (6)
HO1	0.444 (2)	1.096 (3)	0.751 (2)	4.4†
HO3	0.404 (3)	1.159 (4)	0.439 (2)	5.9†
Structure (4)				
Cl	0.58061 (7)	1.00084 (4)	0.84718 (3)	3.532 (9)
O1	0.5995 (2)	0.7673 (1)	0.9472 (1)	4.18 (3)
O2	0.7885 (3)	0.6891 (1)	0.8454 (1)	5.13 (4)
O3	0.8533 (3)	0.3827 (1)	1.0015 (1)	4.55 (3)
N1	0.8584 (2)	0.3359 (1)	0.7992 (1)	2.61 (3)
C1	0.7066 (3)	0.5722 (2)	0.9737 (1)	2.72 (3)
C2	0.8288 (3)	0.4718 (2)	0.9352 (1)	2.74 (3)
C3	0.7285 (2)	0.4162 (2)	0.8553 (1)	2.39 (3)
C4	0.5453 (3)	0.3585 (2)	0.8852 (1)	3.28 (4)
C5	0.4209 (3)	0.4573 (2)	0.9230 (2)	3.87 (4)
C6	0.5120 (3)	0.5255 (2)	0.9991 (1)	3.57 (4)
C7	0.7022 (3)	0.6808 (2)	0.9142 (1)	2.75 (3)
C8	0.7489 (3)	0.2753 (2)	0.7267 (1)	3.97 (4)
C9	1.0040 (4)	0.4123 (2)	0.7548 (2)	4.38 (4)
C10	0.9558 (3)	0.2406 (2)	0.8516 (2)	3.90 (4)
HO1	0.603 (3)	0.819 (2)	0.916 (2)	5.4†
HO3	0.928 (3)	0.413 (2)	1.035 (2)	5.9†

† Fixed at 1.3 times the value of heavy atom to which it is bonded.

Table 2. *Selected geometric parameters* (Å, °)

Structure	(1)[a]	(2)	(3)	(4)
O1—C7	1.324 (10)	1.306 (4)	1.328 (3)	1.313 (2)
O2—C7	1.203 (10)	1.180 (4)	1.199 (3)	1.204 (3)
O3—C2	1.419 (10)	1.406 (3)	1.412 (2)	1.421 (2)
N1—C3	1.518 (10)	1.545 (4)	1.541 (2)	1.542 (2)
N1—C8		1.508 (4)	1.497 (4)	1.500 (3)
N1—C9		1.499 (4)	1.506 (3)	1.502 (3)
N1—C10		1.493 (4)	1.498 (3)	1.498 (3)
C1—C2	1.529 (11)	1.537 (4)	1.540 (3)	1.537 (3)

C1—C6		1.527 (4)	1.528 (4)	1.530 (3)
C1—C7	1.507 (11)	1.523 (4)	1.516 (4)	1.513 (3)
C2—C3	1.519 (11)	1.530 (4)	1.537 (3)	1.529 (2)
C3—C4		1.528 (4)	1.519 (3)	1.524 (3)
C4—C5		1.532 (6)	1.528 (3)	1.529 (3)
C5—C6		1.515 (4)	1.527 (4)	1.520 (3)
C3—N1—C8		109.0 (2)	111.6 (2)	110.4 (1)
C3—N1—C9		110.9 (2)	107.6 (1)	108.8 (1)
C3—N1—C10		112.7 (2)	112.6 (2)	114.2 (1)
C2—C1—C6		111.0 (2)	112.7 (2)	110.8 (1)
C2—C1—C7	111.5 (6)	110.9 (2)	109.0 (2)	112.5 (2)
C6—C1—C7		112.5 (3)	111.2 (2)	113.9 (2)
O3—C2—C1	108.7 (7)	109.3 (2)	113.7 (2)	108.9 (1)
O3—C2—C3	111.3 (7)	112.4 (2)	113.6 (2)	108.4 (1)
C1—C2—C3	107.2 (6)	111.4 (2)	108.6 (2)	109.3 (1)
N1—C3—C2	116.8 (7)	113.2 (2)	112.3 (2)	112.7 (1)
N1—C3—C4		112.7 (2)	112.1 (2)	115.2 (1)
O1—C7—O2	123.3 (8)	122.7 (3)	123.0 (3)	123.4 (2)
O1—C7—C1	111.8 (7)	111.2 (2)	111.5 (2)	112.7 (2)
O2—C7—C1	124.9 (7)	126.2 (3)	125.5 (3)	123.8 (2)
C2—C3—C4		108.4 (2)	112.3 (2)	110.1 (1)
C3—C4—C5		109.1 (3)	108.9 (2)	107.2 (2)
C4—C5—C6		111.6 (3)	110.7 (2)	113.4 (2)
C1—C6—C5		111.8 (2)	110.9 (2)	111.9 (2)
C6—C1—C2—C3		55.0 (3)	−53.6 (2)	56.6 (2)
C7—C1—C2—O3	73.4	53.9 (3)	−50.3 (2)	169.6 (2)
C7—C1—C2—C3	−166.2	−70.9 (3)	−177.6 (2)	−72.1 (2)
C2—C1—C6—C5		−51.4 (3)	54.5 (3)	−51.3 (2)
C2—C1—C7—O2	22.7	50.7 (4)	116.9 (2)	−1.83 (3)
O3—C2—C3—N1	−66.4	51.0 (3)	56.8 (2)	−74.9 (2)
C1—C2—C3—N1	174.8	174.1 (2)	−175.6 (1)	166.4 (1)
C1—C2—C3—C4		−60.1 (3)	57.0 (2)	−63.4 (2)
C2—C3—C4—C5		61.4 (3)	−60.2 (2)	62.2 (2)
C3—C4—C5—C6		−59.5 (3)	58.9 (2)	−57.0 (2)
C4—C5—C6—C1		54.4 (4)	−56.5 (2)	52.7 (2)
Cl···HO1	1.83	2.31 (4)	2.24 (4)	2.30 (3)
Cl···O1	3.00	2.988 (3)	2.973 (2)	3.025 (2)
Cl···HO3	2.23	2.31 (3)	2.40 (3)	5.96 (3)[b]
Cl···O3	3.06	3.168 (2)	3.130 (3)	5.246 (2)[b]
HO1···Cl···HO3	84	95 (1)	100 (1)	
O1···HO1···Cl	169	141 (4)	161 (3)	167 (3)
O3···HO3···Cl	138	168 (3)	153 (3)	

(*a*) Data from Tomita, Urabe, Kim & Fujiwara (1974). (*b*) Distances are much too long for hydrogen bonding.

The space groups for structures (2) ($P2_1/n$) and (4) ($P2_12_12_1$) were uniquely defined by their systematic absences. The space group for structure (3) (*Cc*) was not uniquely defined by the systematic absences but was proven to be correct by the successful structure refinement. The structure solutions and refinements were carried out using *MolEN* (Fair, 1990). Both linear decay corrections and empirical absorption corrections were applied to the data. The chloride ions were located in the Patterson maps and the remainder of the atoms were located by difference Fourier syntheses. All non-H atoms were refined anisotropically. The H atoms were also refined with fixed isotropic thermal parameters. Data were weighted using a non–Poisson scheme with an experimental uncertainty factor of 0.03 for all three structures. A secondary-extinction correction was applied and the extinction coefficient was refined. In the last stage of the refinements, no parameter varied by more than 0.02 of its standard deviation. The final difference Fourier maps had no interpretable peaks. For the noncentrosymmetric space groups of (3) and (4), both enantiomers were refined, and *R*, *wR* and *S* are reported for both refinements. Data and figures are for the enantiomers with the lower values. Corrections for anomalous dispersion were taken from Cromer (1974) and applied to the chloride ions.

ORTEP (Johnson, 1976) plots of (2), (3) and (4) are given in Figs. 1(*a*), 1(*b*) and 1(*c*), respectively. Unit-cell diagrams for (2), (3) and (4) are given in Figs. 2(*a*), 2(*b*) and 2(*c*). Note that, while (1) contains the (2*R*) configuration [numbered as in (2)–(4)], the configurations illustrated in Figs. 1(*a*–*c*) for (2)–(4) are (1*S*,2*S*,3*S*), (1*R*,2*S*,3*S*), and (1*S*,2*R*,3*S*), respectively.

Data collection and cell refinement: *CAD-4 Software* (Enraf–Nonius, 1989). Program used to solve structure: *MolEN* (Fair, 1990). Program used to refine structure: *MolEN*. Molecular graphics: *ORTEP*II (Johnson, 1976). Software used to prepare material for publication: *MolEN*.

This work was supported by a grant (HL44668) to WJB from the National Institutes of Health.

Lists of structure factors, anisotropic displacement parameters, H-atom coordinates and complete geometry have been deposited with the IUCr (Reference: BK1049). Copies may be obtained through The Managing Editor, International Union of Crystallography, 5 Abbey Square, Chester CH1 2HU, England.

References

Brouillette, W. J., Saeed, A., Abuelyaman, A., Hutchison, T. L., Wolkowicz, P. E. & McMillin, J. B. (1994). *J. Org. Chem.* **59**, 4297–4303.

Colucci, W. J. & Gandour, R. D. (1988). *Bioorg. Chem.* **16**, 307–334.

Colucci, W. J., Gandour, R. D. & Mooberry, E. A. (1986). *J. Am. Chem. Soc.* **108**, 7141–7147.

Cromer, D. T. (1974). *International Tables for X-ray Crystallography*, Vol. IV, Table 2.3.1. Birmingham: Kynoch Press. (Present distributor Kluwer Academic Publishers, Dordrecht.)

Cromer, D. T. & Waber, J. T. (1974). *International Tables for X-ray Crystallography*, Vol. IV, Table 2.2B. Birmingham: Kynoch Press. (Present distributor: Kluwer Academic Publishers, Dordrecht.)

Enraf–Nonius (1989). *CAD-4 Software*. Version 5.0. Enraf–Nonius, Delft, The Netherlands.

Fair, C. K. (1990). *MolEN. An Interactive Intelligent System for Crystal Structure Analysis*. Enraf–Nonius, Delft, The Netherlands.

Johnson, C. K. (1976). *ORTEP*II. Report ORNL-5138. Oak Ridge National Laboratory, Tennessee, USA.

Tomita, K., Urabe, K., Kim, Y. B. & Fujiwara, T. (1974). *Bull. Chem. Soc. Jpn*, **47**, 1988–1993.

Zachariasen, W. H. (1963). *Acta Cryst.* **16**, 1139–1144.

Acta Cryst. (1995). C**51**, 1164–1167

4,4′-Azoxydianisole at 203 K

Chafic Chebli and François Brisse

Département de Chimie, Université de Montréal, CP 6128, Succursale Centre-ville, Montréal, Québec, Canada H3C 3J7

(*Received* 29 *August* 1994; *accepted* 25 *October* 1994)

Abstract

The crystal structure determination of the title compound, $C_{14}H_{14}N_2O_3$, reinvestigated using low-

Contrasting effects of propionate and propionyl-L-carnitine on energy-linked processes in ischemic hearts

FABIO DI LISA, ROBERTA MENABÒ, ROBERTA BARBATO, AND NORIS SILIPRANDI
Dipartimento di Chimica Biologica, Università di Padua and Centro Studio Fisiologia Mitocondriale, Consiglio Nazionale delle Ricerche, 35121 Padua, Italy

Di Lisa, Fabio, Roberta Menabò, Roberta Barbato, and Noris Siliprandi. Contrasting effects of propionate and propionyl-L-carnitine on energy-linked processes in ischemic hearts. *Am. J. Physiol.* 267 (*Heart Circ. Physiol.* 36): H455–H461, 1994.—Propionyl-L-carnitine, unlike L-carnitine, is known to improve myocardial function and metabolism altered during the course of ischemia-reperfusion. In this study, the effect of propionyl-L-carnitine has been compared with that of propionate and carnitine on the performance of rat hearts perfused with a glucose-containing medium either under normoxia, ischemia, or postischemic reperfusion. In the postischemic phase, contractile parameters were partially restored both in the control and in the propionate plus carnitine-treated hearts, were markedly impaired by propionate, and were fully recovered by propionyl-L-carnitine. In addition, propionyl-L-carnitine, but not propionate, reduced the functional decay of mitochondria prepared from the ischemic hearts. Even in normoxic conditions propionate, unlike propionyl-L-carnitine, caused a drastic reduction of free CoA and L-carnitine. The concomitant increase in lactate production and decrease in ATP content might be explained by the inhibition of pyruvate dehydrogenase caused by the accumulation of propionyl-CoA. Indeed, when pyruvate was the only oxidizable substrate, propionate induced a gradual decrease in developed pressure, which was largely prevented by L-carnitine. The protective effect of propionyl-L-carnitine may be a consequence of the anaplerotic utilization of propionate in the presence of an optimal amount of ATP and free L-carnitine.

ischemia; mitochondria; L-carnitine; coenzyme A

PROPIONYL-L-CARNITINE (PLC) and L-carnitine (carnitine) are both known to protect the ischemic myocardium under various experimental conditions (6, 8, 13, 18, 20, 24), but the ester is the more effective (6, 18, 20). PLC also has a beneficial action on peripheral arterial disease, which is not shared by carnitine (2). Two explanations, not mutually exclusive, have been proposed for these differences. As well as releasing carnitine inside mitochondria, PLC could act as an anaplerotic substrate, boosting the level of intermediates in the tricarboxylic acid (TCA) cycle by supplying propionyl moieties (6), which are easily convertible, via methylmalonyl-CoA, into succinate. It could also penetrate more readily than carnitine (20).

A clearer picture of the actual mechanism would be obtained by comparing the effect of PLC with that of propionate, alone or mixed with carnitine, all under identical experimental conditions. So far, this has only been done with rabbits in which PLC was specific in improving the contractile performance of isolated hearts (9). Both PLC and carnitine increased the endogenous carnitine content to the same extent, but propionate was lethally toxic (9). This was in agreement with an earlier report that propionate depresses the mechanical function of isolated working hearts under normoxic conditions (1), whereas PLC aids recovery after ischemia (8, 13, 18, 20).

In the present study we have compared the metabolic effects of propionate and PLC on rat hearts exposed to ischemia and postischemic reperfusion. We show that they have different effects not only on cardiac performance but also on the properties of mitochondria isolated from the perfused hearts and on the myocardial concentrations of short-chain esters of CoA and of carnitine.

METHODS

Heart perfusion. Hearts were rapidly excised from fed adult male Wistar rats (220–250 g body weight). They were perfused by the nonrecirculating Langendorff technique, using a modified Krebs-Henseleit solution with 11 mM glucose as substrate in a medium containing (in mM) 115 NaCl, 4.0 KCl, 1.5 $CaCl_2$, 1.1 $MgSO_4$, 25.0 $NaHCO_3$, and 0.9 KH_2PO_4. The buffer was gassed with 95% O_2–5% CO_2 to give a Po_2 > 600 mmHg and a final pH of 7.4. This medium was delivered to the aortic cannula by means of a peristaltic pump. During normoxic perfusions, the flow was maintained at 10 ml/min for 20 min before ischemia and for 30 min afterwards. Ischemia was induced by reducing the flow rate to 0.2 ml/min for 90 min. These conditions were chosen by trial and error to minimize irreversible damage. Left ventricular wall temperature was maintained at 36–37°C irrespective of coronary flow by suspending the heart in a water-jacketed chamber. The effluent was discarded except when the release of metabolites was to be studied. In that case, a normoxic recirculating system was used with a total perfusate volume of 90 ml. The hearts were placed in the recirculating system after a 20-min equilibration without recirculation. During recirculation, the contractile activity remained stable for > 90 min. Electrical stimulation of the hearts was achieved using suprathreshold rectangular 0.1-ms pulses delivered from a Tektronix square-wave generator assembly at 5 Hz. Threshold was determined by slowly increasing the stimulator voltage until capture occurred (< 2-V impulse). The voltage was then adjusted to 0.5 V above this level.

To obtain an isovolumetrically beating preparation, a saline-filled latex balloon, connected via a catheter to a Statham transducer (P-2306), was inserted into the left ventricle through an atriotomy and secured with suture around the atrioventricular groove (9). Normally, the balloon was inflated to provide an end-diastolic pressure < 5.0 mmHg. Two three-way stopcocks between the transducer, syringe, and the tube leading to the heart allowed for continuous monitoring of left ventricular developed pressure recorded by a Hewlett-Packard HP7754A thermal-tip recorder.

Metabolite assay. For tissue analysis, the hearts were freeze-clamped with alumina tongues cooled in liquid nitrogen. Freeze-clamped tissue (0.3 g, stored at −70°C) was ground and mixed thoroughly with 1 ml of 14% (vol/vol) $HClO_4$ containing 2 mM dithiothreitol (DTT) to allow as well the estimates of

CoA derivatives, all at −130°C (9). The mixture was transferred from the mortar to a tube and allowed to thaw while stirred on a Vortex mixer. It was further homogenized four times at 0–4°C with an ultra-turrax for 3–5 s, interspaced with 30-s cooling periods. After centrifugation, the pellet was washed three times. The collected supernatant fluids containing acid-soluble metabolites were pooled and used for the assay of CoA and carnitine. Long-chain acyl esters of CoA and carnitine (acid-insoluble metabolites) were determined in the pellets.

The neutralized extracts were assayed radioenzymatically for their carnitine concentrations (17), either directly (free carnitine) or after alkaline hydrolysis (15 min at pH 10, 55°C). The difference represents the contribution of short-chain acylcarnitines (SCAC) to the total carnitine concentration. SCAC fractions were also separated and quantitated as previously described (9). Briefly, after the enzymatic exchange of [^{3}H]carnitine with the acylcarnitine pool of the sample, individual acylcarnitines were measured by reverse-phase high-performance liquid chromatography (HPLC) coupled to an instream continuous flow through a Radiomatic β-counter. Free CoA was assayed with an enzymatic cycling method (28). Acid-soluble CoA fractions were assayed by an HPLC method (6). With the use of a digital-digital interface coupled to a dedicated software system (System Gold, Beckman), the peaks of interest were identified and quantified by comparison with a standard curve of authentic short-chain acyl-CoA esters.

Long-chain acyl esters were determined as free CoA or carnitine released after the alkaline hydrolysis of the perchloric acid-insoluble pellet (9).

Lactate was determined in the coronary effluent using a classic enzymatic assay (10).

Adenine nucleotides were assayed in the neutralized perchloric extracts with an HPLC method as previously described (9). Phosphocreatine (PCr) was assayed enzymatically (11).

Mitochondrial function. Mitochondria were isolated by conventional procedures of differential centrifugation (14). Hearts were homogenized in a medium containing 0.13 M KCl, 10 mM EDTA, 0.5% albumin, 10 mM *N*-2-hydroxyethylpiperazine-*N*′-2-ethanesulfonic acid (HEPES), pH 7.4. To remove EDTA and albumin, mitochondrial pellets were washed twice with 0.13 M KCl, 10 mM HEPES, pH 7.4 (9). Membrane potential ($\Delta\psi$) was measured with tetraphenylphosphonium (TPP^+)-selective electrode (6). Incubations were carried out at 20°C with 0.5 mg mitochondrial protein/ml in the following standard medium: 0.2 M sucrose, 10 mM HEPES, pH 7.4, 5 mM succinate, 1.25 μM rotenone. The total incubation volume was 3 ml.

Statistics. Data are expressed as means ± SE of at least six experiments, with each experiment being an individual perfusion. One-way analysis of variance was first carried out to test for any differences between all groups. If a difference was established, each of the groups was compared with the saline control group using the Student's unpaired *t* test, considering differences with $P < 0.05$ significant.

The reagents were analytic compounds of the highest grade available. All enzymes used for the biochemical determinations were obtained from Sigma (St. Louis, MO). Carnitine and PLC were supplied by Sigma-Tau (Rome, Italy).

RESULTS

Diastolic and developed pressures of unstimulated perfused rat hearts have been measured in the presence of either carnitine, PLC, or propionate before and after ischemia induced by reducing the perfusion flow rate (Fig. 1). Figure 2 shows the mean values of developed and diastolic left ventricular pressures of the same groups during postischemic reperfusion.

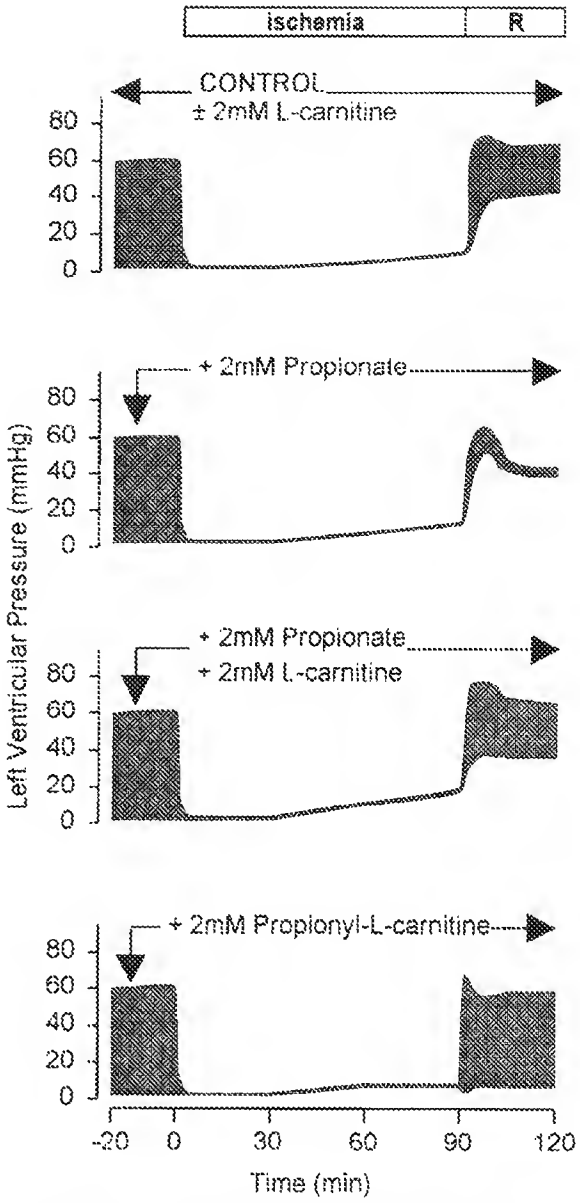

Fig. 1. Graphic representation of mean values of ventricular pressures of perfused unstimulated rat hearts. *R*, reperfusion.

In the preischemic phase, neither the pressures nor the frequency of contractions was affected by the additions (not shown). In all groups the reduction of coronary flow induced a rapid contractile failure, and cessation of beating occurred in <2 min. Twenty to forty minutes after the reduction of flow, diastolic pressure started to increase, reaching similar values in all groups (15 ± 5 mmHg) at the end of the ischemic phase.

On subsequent reperfusion, the control group demonstrated a sudden increase in the diastolic pressure associated with a partial recovery of contractile activity. In the presence of propionate, although there was a similar increase in the diastolic pressure, it was accompanied by only a slight recovery of the developed pres-

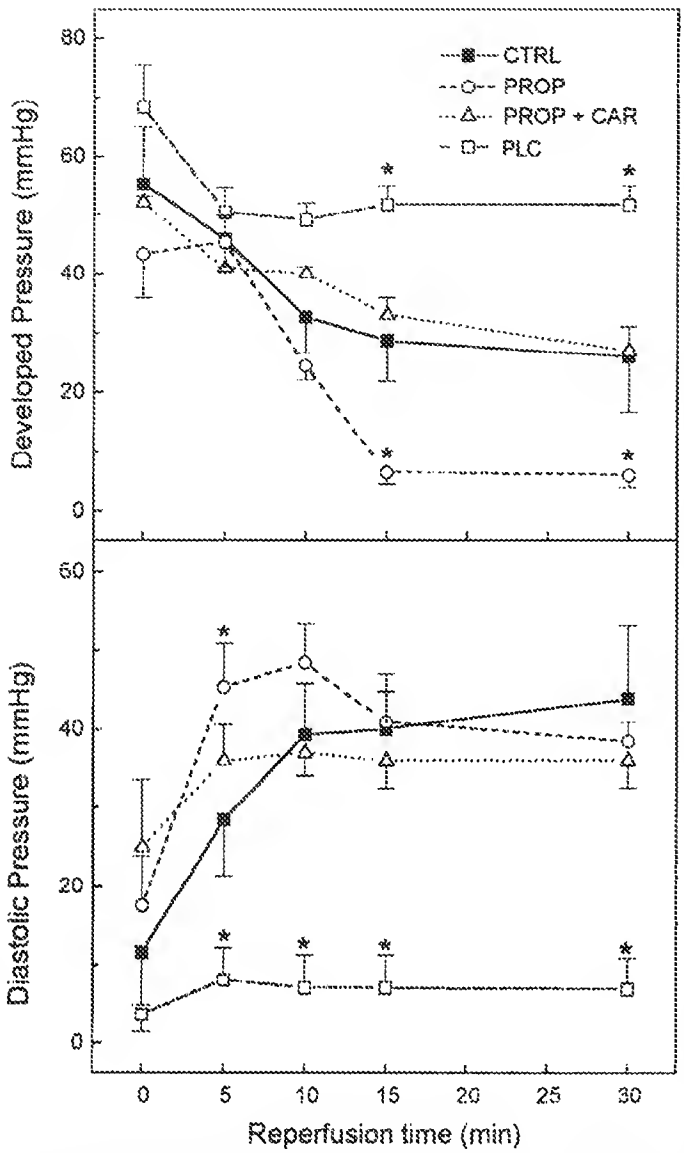

Fig. 2. Effect of postischemic reperfusion on developed and diastolic pressure of perfused rat hearts. Values are means ± SE of 6 experiments. Prop, propionate (2 mM); Car, L-carnitine (2 mM); PLC, propionyl-L-carnitine (2 mM). *$P < 0.05$ statistical difference between treated and untreated [control (Ctrl)] hearts.

sure. The group with carnitine plus propionate behaved in the same way as the control group.

In contrast, when PLC was added alone, reperfusion was accompanied by an almost complete recovery of the preischemic contractile parameters. At the end of the reflow phase, diastolic pressure did not show any rise with respect to the ischemic values, and developed pressure was significantly higher than in the control group.

We next determined the energy-linked properties of mitochondria isolated from the hearts at the end of normoxic and ischemic perfusions (Fig. 3).

Mitochondria isolated from ischemic hearts showed changes in $\Delta\psi$ compared with those isolated from normoxic hearts perfused with the same substrate. In each case there was a lower steady-state $\Delta\psi$ (147 ± 6 and 164 ± 5 mV), a smaller decrease of $\Delta\psi$ on ADP addition (22 ± 4 vs. 33 ± 5 mV), and a slower rate of return to the new steady state after ADP addition. Thus both transmembrane potential and the efficiency of oxidative phosphorylation were significantly impaired by ischemia. These deficiencies due to anoxia were not significantly affected by the presence of propionate, with or without carnitine, in the heart perfusion medium but were considerably amended by PLC.

The distribution of CoA and its esters in these normoxic and ischemic hearts is reported in Table 1.

In the normoxic control, much of the CoA was present in the free form. After normoxic perfusion with propionate, this was drastically reduced, but in compensation, there was a more than twofold increase in its esters, most strikingly in the acid-soluble propionyl-CoA and methylmalonyl-CoA (almost absent in the normoxic controls), but also in long-chain acyl-CoA (LCACoA) esters. With carnitine also present, this CoA-trapping effect of propionate was much less.

The perfusion with PLC in normoxic conditions resulted in an almost complete preservation of free CoA and in a significantly lower accumulation of both short-chain acyl-CoA (SCACoA) and LCACoA with respect to propionate. Methylmalonyl-CoA, which can be considered the metabolic hallmark of a large propionate supply, was not detectable in PLC-perfused hearts. As in the case of propionate, propionyl-CoA was the prevalent ester among SCACoA.

Irrespective of the treatments, ischemia induced a large accumulation of LCACoA. Even under ischemic conditions, free CoA was significantly higher in PLC-treated hearts than in the propionate group.

Table 2 shows the content of carnitine fractions of normoxic and ischemic hearts perfused either in the presence or in the absence of propionate. Both in normoxic and ischemic conditions, propionate induced a marked decrease of free carnitine and a concurrent increase of SCAC. In ischemic conditions, a considerable increase of long-chain acylcarnitine (LCAC) was consistently observed. The changes in carnitine fractions were parallel to those of CoA fractions, as expected by the equilibrium between the CoA and carnitine pools. The groups receiving carnitine or PLC have not been considered in Table 2, since in the presence of massive amounts of exogenous carnitines the evaluation of endogenous ones appeared unreliable.

ATP and PCr contents of the normoxic hearts were significantly decreased by propionate (Table 3). Ischemia induced a fall in ATP and PCr and a rise in AMP levels of similar magnitude in all groups (Table 3).

Despite the large diminution of free CoA and carnitine, an unfavorable condition for mitochondrial energy production, addition of propionate to the perfusion medium did not affect the contractile power under normoxic conditions. This indicates that glycolysis alone can sustain the contractile activity. Such a possibility is supported by the observation (unpublished results) that with glucose as a substrate heart contractility persisted after the addition of rotenone, albeit with decreases in

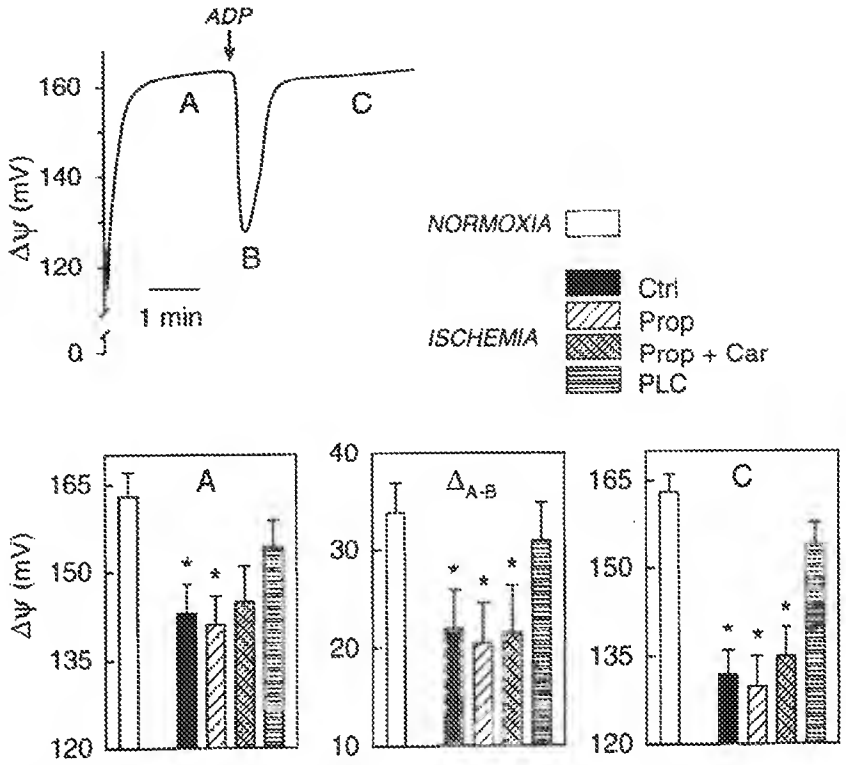

Fig. 3. Effect of ischemia on membrane potential ($\Delta\psi$) of mitochondria from isolated and perfused rat hearts. *Top*: typical behavior of $\Delta\psi$ in normal and well-coupled mitochondria. From steady state (*A*), $\Delta\psi$ falls to a minimum on adding ADP (*B*) but rises again to a new steady state after its conversion to ATP (*C*). *Bottom*: $\Delta\psi$ values at these places for mitochondria isolated after normoxic or ischemic perfusions (see METHODS). Values are means ± SE of 6 experiments. $^*P < 0.05$ statistical difference between ischemic and normoxic mitochondria.

both the heart rate (from 240 ± 20 to 80 ± 9 beats/min) and the developed pressure (from 67 ± 5 to 38 ± 7 mmHg).

Further evidence for the impairment of mitochondrial oxidative processes is provided by the results in Fig. 4. The time course of lactate release into perfusate indicates that even in normoxic conditions addition of propionate inhibited pyruvate oxidation. Carnitine added together with propionate significantly delayed the increased rate of lactate production.

Considering that propionate traps free CoA (see Table 1) and that carnitine, through the action of carnitine acetyl transferase, reduces the extent of this trapping, the inhibition of pyruvate dehydrogenase can be attributed to the high propionyl-CoA-to-CoA ratio created by propionate loading. PLC did not result in a noticeable production of lactate, which as expected, was stimulated by the subsequent addition of rotenone.

When glycolysis was inhibited by iodoacetate and acetate was added as the respiratory substrate, no lactate was formed either in the presence or absence of propionate, showing that the latter could not itself be a lactate precursor (26) in our system. Under these conditions, the mechanical activity was unchanged.

The view that glycolysis alone drives the heart contractions in the presence of propionate was tested directly by measuring left ventricular pressure using pyruvate as substrate and preincubating with iodoacetate to inhibit glycogenolysis (Fig. 5). In unstimulated hearts, propionate gradually decreased the contractile frequency, eventually leading to complete systolic arrest (results not shown). For this reason, hearts were paced with electrical stimulation to maintain an appreciable and constant rate of energy demand, then the gradual decrease in developed pressure due to propionate followed until cardiac arrest. This decline was largely prevented by carnitine such that, even 1 h later, mechanical activity remained without major diastolic change. Under these conditions, contractile activity was unaffected by PLC (results not shown).

Table 1. *Free CoA and acyl-CoA contents in isolated rat hearts*

	Free	SCACoA	LCACoA	Acetyl-CoA	Succinyl-CoA	Propionyl-CoA	Metmal-CoA
Normoxia							
Control	46.7 ± 3.9	19.0 ± 2.6	12.7 ± 2.7	4.6 ± 1.5	13.2 ± 2.0	1.0 ± 0.8	
Prop	6.93 ± 1.3*	51.2 ± 5.7*	20.5 ± 4.0*	0.3 ± 0.2*	2.6 ± 1.0*	19.8 ± 2.9*	28.5 ± 1.1*
Prop + Carn	29.0 ± 2.2*	32.4 ± 3.8*	11.9 ± 2.4	2.8 ± 0.7*	7.2 ± 1.9*	14.0 ± 4.2*	9.5 ± 2.4*
Propionyl-L-carnitine	37.6 ± 4.6	27.9 ± 3.3*	17.7 ± 2.7	1.8 ± 0.5*	13.3 ± 3.1	11.1 ± 2.7*	
Ischemia							
Control	30.1 ± 2.0	12.5 ± 2.7	49.7 ± 6.6	4.8 ± 1.3	7.7 ± 1.3	1.0 ± 0.6	
Prop	10.1 ± 1.8*	28.0 ± 3.0*	46.5 ± 6.2	0.2 ± 0.1*	7.2 ± 3.2	10.8 ± 4.9*	9.8 ± 5.2*
Prop + Carn	18.5 ± 2.3*	34.3 ± 0.9*	44.6 ± 5.9	1.8 ± 0.3*	9.8 ± 1.7	6.8 ± 1.0*	6.8 ± 1.5*
Propionyl-L-carnitine	24.1 ± 3.1	17.7 ± 4.9	41.1 ± 5.5	1.0 ± 0.3*	6.9 ± 4.3	9.6 ± 1.9*	

Values (nmol/g wet weight) are means ± SE; $n = 6$ hearts. Free, unesterified CoA; SCACoA, short-chain acyl-CoA; LCACoA, long-chain acyl-CoA; Metmal-CoA, methylmalonyl-CoA; Prop, propionate; Carn, carnitine. $^*P < 0.05$ vs. control.

Table 2. *Free carnitine and acylcarnitine contents in isolated rat hearts*

	Free	SCAC	LCAC
Normoxia			
Control	661.3 ± 29.9	85.1 ± 7.0	38.5 ± 3.8
Prop	276.0 ± 39.4*	471.3 ± 31.2*	40.4 ± 4.1
Ischemia			
Control	503.3 ± 6.1	87.9 ± 1.7	216.6 ± 12.6
Prop	311.6 ± 32.0*	329.3 ± 34.5*	135.3 ± 5.8*

Values (nmol/g wet weight) are means ± SE; n = 6 hearts. SCAC, short-chain acylcarnitine; LCAC, long-chain acylcarnitine. *P < 0.05 vs. control.

DISCUSSION

Our results show that propionate augments, whereas PLC diminishes, the adverse effects of ischemia on perfused hearts. The explanation for this difference is to be sought in the properties of the subsequently isolated mitochondria from these hearts.

Propionate is known to deplete mitochondrial ATP (3) by converting it into AMP during the formation of propionyl-CoA (see Table 1). Although AMP also inhibits the intramitochondrial ATP-dependent thiokinase (25), it itself easily disappears from the matrix after degradation (4), resulting in an irreversible depletion of the mitochondrial nucleotide pool.

We have shown that propionate depletes both free CoA and free carnitine and reduces ATP content significantly. The resulting increased propionyl-CoA-to-CoA ratio would depress the activity of the α-ketoacid dehydrogenases and hence the flux through the TCA cycle. In particular, inhibition of α-ketoglutarate dehydrogenase blocks the only mitochondrial route for the rephosphorylation of AMP to ATP at the substrate level (21). Consequently, the reduced utilization of α-keto acids, mainly pyruvate and α-ketoglutarate, may impair maintenance of normal $\Delta\psi$. Although the addition of carnitine does not circumvent the expenditure of ATP required for propionate activation, it does, however, prevent the decrease of ATP and PCr induced by propionate; thus this decrease appears to be mainly determined by the dehydrogenase inhibition.

Table 3. *Adenine nucleotide and phosphocreatine contents in isolated rat hearts*

	ATP	ADP	AMP	PCr
Normoxia				
Control	2.56 ± 0.12	0.69 ± 0.05	0.21 ± 0.01	3.51 ± 0.18
Prop	1.79 ± 0.23*	0.84 ± 0.14	0.32 ± 0.07	1.94 ± 0.34*
Prop + Carn	2.61 ± 0.11	0.62 ± 0.06	0.20 ± 0.02	3.58 ± 0.21
Propionyl-L-carnitine	2.46 ± 0.08	0.66 ± 0.03	0.27 ± 0.03	3.39 ± 0.26
Ischemia				
Control	0.76 ± 0.04	0.62 ± 0.03	0.98 ± 0.08	0.59 ± 0.09
Prop	0.74 ± 0.13	0.64 ± 0.06	0.87 ± 0.09	0.55 ± 0.05
Prop + Carn	0.71 ± 0.11	0.59 ± 0.01	0.97 ± 0.06	0.53 ± 0.07
Propionyl-L-carnitine	0.69 ± 0.06	0.55 ± 0.07	0.93 ± 0.11	0.62 ± 0.07

Values (μmol/g wet weight) are means ± SE; n = 6 hearts. PCr, phosphocreatine. *P < 0.05 vs. control.

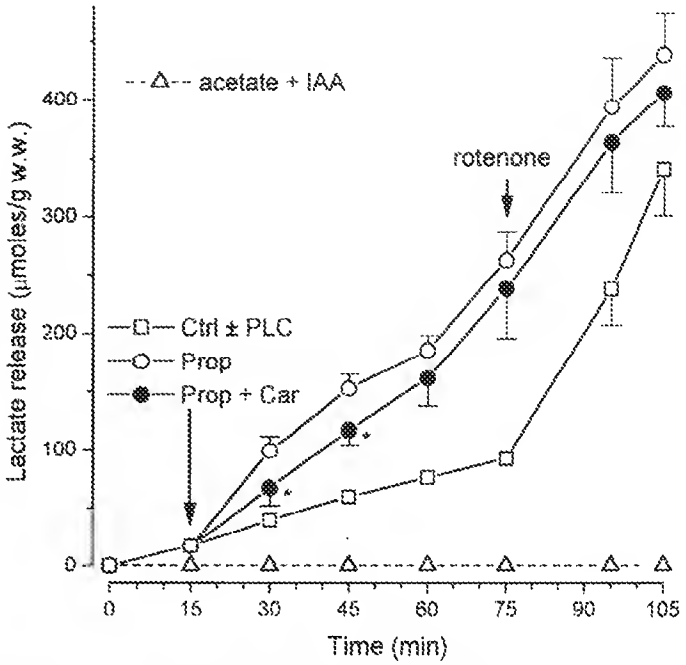

Fig. 4. Time course of lactate release in isolated hearts perfused under normoxic conditions. Perfusions with glucose (11 mM)-containing medium (see METHODS) are indicated by solid lines. Arrows indicate addition of indicated substances to perfusion media. Dashed line refers to hearts perfused with 1 mM acetate in absence of glucose. Iodoacetate (IAA, 0.15 mM) was also present to inhibit glycolysis. Values are means ± SE of 6 experiments. Rotenone concentration, 2 μM. *P < 0.05 statistical difference between propionate and propionate + carnitine-treated hearts.

Although the propionyl moiety of PLC is also transferred to produce propionyl-CoA, it differs from propionate activation in that it does not consume ATP (3). Extra free carnitine is of course produced by the transfer and, as we have also found, PLC does not deplete free CoA to the same extent, possibly because of a slower

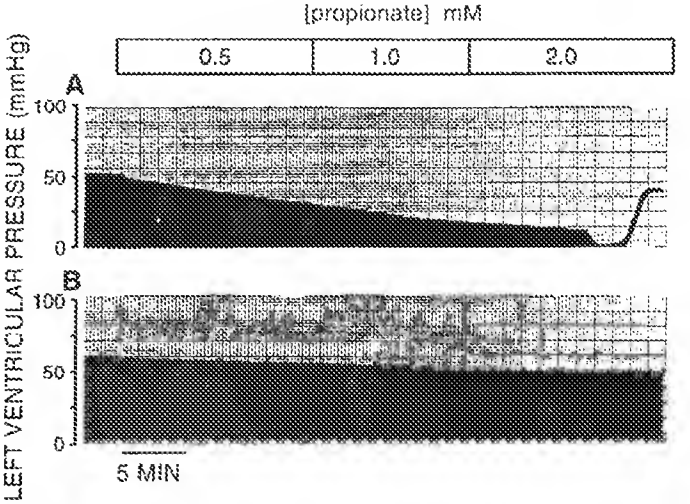

Fig. 5. Traces showing contractility of isolated rat hearts perfused under normoxic conditions with increasing concentrations of added propionate without (*A*; control) and with (*B*) carnitine (2 mM). For this experiment, pyruvate (1 mM) replaced glucose, and 0.15 mM iodoacetate was added to inhibit glycolysis. Propionate was added at time and quantities shown. Similar traces were obtained in 2 other experiments.

utilization due to the different rates of propionate and PLC transport across cellular membranes.

We suggest that the lowered tissue ATP plus free CoA and the increased LCACoA esters create unfavorable conditions, which worsen the ischemic injury. These impairments in energy metabolism may in turn be responsible for the decline in cardiac contractility observed during reperfusion.

Other literature supports this view. In working hearts perfused with acetoacetate (22, 23), a decrease in free CoA was linked with a fall in TCA cycle intermediates induced by inhibition of α-ketoglutarate dehydrogenase. Propionate was also found to affect cardiac performance in working hearts, even under aerobic conditions and in the presence of glucose (1). In our conditions, Langendorff-perfused hearts, in which oxidative metabolic rates are lower than in working hearts, propionate produced "mitochondrial insufficiency," which became particularly evident when glucose was replaced by pyruvate in the perfusing medium. This decline in mechanical activity is attributed to the inhibition of pyruvate oxidation by the formed propionyl-CoA, which is a potent inhibitor of pyruvate dehydrogenase (15).

Direct evidence for this inhibition is the stimulation of lactate production by propionate. Counteraction by carnitine, which converts the formed propionyl-CoA into the noninhibitory PLC, shows the determinant role of a high propionyl-CoA-to-CoA ratio. When this is achieved, the ATP formed by anaerobic glycolysis in the cytosol appears sufficient, at least for the time span of our experiments, to support the mechanical activity of our perfused hearts. Only on inhibition of anaerobic glycolysis (by iodoacetate) does cardiac contractility by propionate become impaired. In the presence of glucose, the alternative condition for the manifestation of this propionate-damaging action is ischemia (see above).

Mitochondrial $\Delta\psi$ can be generated and maintained, either anaerobically or with inadequate substrate flux, by the glycolytic ATP via reversal of the adenosinetriphosphatase reaction (16) as demonstrated in anoxic myocytes (7) and in isolated hepatocytes treated with oligomycin (27). The increase in LCACoA esters that we observed might be expected to interfere with this process by preventing the translocation of ATP between cytosol and mitochondria (19). Because mitochondria are involved in cellular Ca^{2+} handling (12), a partial collapse of mitochondrial $\Delta\psi$ could perturb the ionic balance of the cells (5).

Unlike propionate, PLC has a negligible effect on mitochondrial energy-linked processes and hence does not impair postischemic contractility. In fact, the results show that it somewhat increases it (see Fig. 1) This stimulation may be due to the increased supply of mitochondrial carnitine donated by PLC and the consequent increase in propionyl-CoA. The latter is, of course, convertible to succinate and may stimulate the TCA cycle anaplerotically by adding to the pool of intermediates. Despite an analogous anaplerotic action, propionate significantly hampered mitochondrial efficiency. Conceivably, free CoA and ATP deprivation nullifies the favorable effects of anaplerosis on mitochondrial energy-linked processes. Obviously, the involvement of mitochondrial function in PLC effects does not exclude other mechanisms. Ultimately, it is likely that the protective action exerted by PLC might result from a positive interplay between *1*) improved mitochondrial function in myocytes, *2*) iron chelation (18), and *3*) preservation of vascular patency (2, 24).

The authors thank Prof. Peter Jocelyn and Dr. Alison Cessario for the critical reading of the manuscript.

This work was supported by Consiglio Nazionale delle Ricerche target project Biotecnologie e Biostrumentazione (Grant 9201257; PF 70) and Sigma-Tau (Pomezia, Italy).

Address for reprint requests: F. Di Lisa, Dipartimento di Chimica Biologica, Via Trieste, 75, 35121 Padua, Italy.

Received 24 September 1993; accepted in final form 14 March 1994

REFERENCES

1. **Bolukoglu, H., S. H. Nellis, and A. J. Liedtke.** Effects of propionate on mechanical and metabolic performance in aerobic rat hearts. *Cardiovasc. Drugs Ther.* 5, *Suppl. 1*: 37–44, 1991.
2. **Brevetti, G., S. Perna, C. Sabba, A. Rossini, V. Scotto di Uccio, E. Berardi, and L. Godi.** Superiority of L-propionylcarnitine vs. L-carnitine in improving walking capacity in patients with peripheral vascular disease: an acute, intravenous, double-blind, cross-over study. *Eur. Heart J.* 13: 251–255, 1992.
3. **Ciman, M., C. R. Rossi, and N. Siliprandi.** On the mechanism of the antiketogenic action of propionate and succinate in isolated rat liver mitochondria. *FEBS Lett.* 22: 8–10, 1972.
4. **de Groot, M. J. M., W. A. Coumans, and G. J. van der Vusse.** The nucleotide metabolism in lactate perfused hearts under ischaemic and reperfused conditions. *Mol. Cell. Biochem.* 118: 1–14, 1992.
5. **Di Lisa, F., G. Gambassi, H. Spurgeon, and R. G. Hansford.** Intramitochondrial free Ca^{2+} in cardiac myocytes in relation to dehydrogenase activation. *Cardiovasc. Res.* 27: 1840–1844, 1993.
6. **Di Lisa, F., R. Menabò, and N. Siliprandi.** L-Propionylcarnitine protection of mitochondria in ischemic rat hearts. *Mol. Cell. Biochem.* 88: 169–173, 1989.
7. **Di Lisa, F., H. Silverman, M. D. Stern, P. S. Blank, G. Gambassi, and R. G. Hansford.** Effect of anoxia and reoxygenation on mitochondrial membrane potential of single cardiac myocytes (Abstract). *Circulation* 86: 1–35, 1992.
8. **Ferrari, R., C. Ceconi, S. Curello, E. Pasini, and O. Visioli.** Protective effect of propionyl-L-carnitine against ischaemia and reperfusion-damage. *Mol. Cell. Biochem.* 88: 161–168, 1989.
9. **Ferrari, R., F. Di Lisa, J. W. De Jong, C. Ceconi, E. Pasini, R. Barbato, R. Menabò, M. Barbieri, E. Cerbai, and A. Mugelli.** Prolonged propionyl-L-carnitine pretreatment of rabbit: biochemical, hemodynamic and electrophysiological effects on myocardium. *J. Mol. Cell. Cardiol.* 24: 219–232, 1992.
10. **Gutman, I., and A. W. Wahlefeld.** L-(+)-Lactate. Determination with lactate dehydrogenase and NAD. In: *Methods of Enzymatic Analysis*, edited by H. U. Bergmeyer. Deerfield, FL: Weinheim, 1974, vol. 3, p. 1464–1468.
11. **Heinz, F., and H. Weißer.** Creatine phosphate. In: *Methods of Enzymatic Analysis*, edited by H. U. Bergmeyer. Deerfield, FL: Weinheim, 1985, vol. 8, p. 507–514.
12. **Lenzen, S., R. Bickthier, and V. Panten.** Interaction between spermine and Mg^{2+} on mitochondrial Ca^{2+} transport. *J. Biol. Chem.* 261: 16478–16483, 1986.
13. **Liedtke, A. J., L. Demaison, and S. H. Nellis.** Effects of L-propionylcarnitine on mechanical recovery during reflow in intact hearts. *Am. J. Physiol.* 255 (*Heart Circ. Physiol.* 24): H169–H176, 1988.
14. **Lindenmayer, G. E., L. A. Sordahl, and A. Schwartz.** Reevaluation of oxidative phosphorylation in cardiac mitochondria from normal animals and animals in heart failure. *Circ. Res.* 23: 439–450, 1968.
15. **Matsuishi, T., D. A. Stumpf, M. Seliem, L. A. Eugren, and K. Chrislip.** Propionate mitochondrial toxicity in liver and skeletal muscle: acyl CoA levels. *Biochem. Med. Metab. Biol.* 45: 244–253, 1991.

16. **Nicholls, D. G., and S. J. Ferguson.** *Bioenergetics* 2. London: Academic, 1992.
17. **Noel, H., R. Parvin., and S. V. Pande.** [gamma]-Butyrobetaine in tissues and serum of fed and starved rats determined by an enzymic radioisotopic procedure. *Biochem. J.* 220: 701–706, 1984.
18. **Packer, L., M. Valenza, E. Serbinova, P. Starke-Reed, K. Frost, and V. Kagan.** Free radical scavenging is involved in the protective effect of L-propionylcarnitine against ischemia-reperfusion injury of the heart. *Arch. Biochem. Biophys.* 288: 533–537, 1991.
19. **Pande, S. V., and M. C. Blanchaer.** Reversible inhibition of mitochondrial adenosine diphosphate phosphorylation by long chain coenzyme A esters. *J. Biol. Chem.* 246: 402–411, 1971.
20. **Paulson, D. J., J. Traxler, M. Schmidt, J. Noonan, and A. L. Shug.** Protection of the ischaemic myocardium by L-propionylcarnitine: effects on the recovery of cardiac output after ischaemia and reperfusion, carnitine transport, and fatty acid oxidation. *Cardiovasc. Res.* 20: 536–541, 1986.
21. **Rossi, C. R., A. Alexandre, G. Carignani, and N. Siliprandi.** The role of mitochondrial adenine nucleotide pool on the regulation of fatty acid and α-ketoglutarate oxidation. *Adv. Enzyme Regul.* 10: 171–186, 1972.
22. **Russell, R. R., III, and H. Taegtmeyer.** Changes in citric acid cycle flux and anaplerosis antedate the functional decline in isolated rat hearts utilizing acetoacetate. *J. Clin. Invest.* 87: 384–390, 1991.
23. **Russell, R. R., III, and H. Taegtmeyer.** Coenzyme A sequestration in rat hearts oxidizing ketone bodies. *J. Clin. Invest.* 89: 968–973, 1992.
24. **Sassen, L. M., K. Bezstarosti, W. J. van der Giessen, J. M. J. Lamers, and P. D. Verdouw.** L-Propionylcarnitine increases postischemic blood flow but does not affect recovery of energy charge. *Am. J. Physiol.* 261 (*Heart Circ. Physiol.* 30): H172–H180, 1991.
25. **Scholte, H. R., E. M. Wit-Peeters, and J. C. Bakker.** The intracellular and intramitochondrial distribution of short-chain acyl-CoA synthetase in guinea pig heart. *Biochim. Biophys. Acta* 231: 479–486, 1971.
26. **Sherry, A. D., C. R. Malloy, R. E. Roby, A. Rajagopal, and F. M. Jeffrey.** Propionate metabolism in the rat heart by ^{13}C-NMR spectroscopy. *Biochem. J.* 254: 593–598, 1988.
27. **Snyder, J. W., J. G. Pastorino, A. P. Thomas, J. B. Hoek, and J. L. Farber.** ATP synthase activity is required for fructose to protect cultured hepatocytes from the toxicity of cyanide. *Am. J. Physiol.* 264 (*Cell Physiol.* 33): C709–C714, 1993.
28. **Veloso, D., and R. L. Veech.** Stoichiometric hydrolysis of long chain acyl-CoA and measurement of the CoA formed with an enzymatic cycling method. *Anal. Biochem.* 62: 449–460, 1974.